5-1-2008

Integrated optical fiber laser Raman sensor for cryogenic application

Appolinaire Tifang Luanje

INTEGRATED OPTICAL FIBER LASER RAMAN SENSOR

FOR CRYOGENIC APPLICATION

By

Appolinaire Tifang Luanje

A Thesis
Submitted to the Faculty of
Mississippi State University
in Partial Fulfillment of the Requirements
for the Degree of Master of Science in Physics
in the Department of Physics and Astronomy

Mississippi State, Mississippi

May 2008

INTEGRATED OPTICAL FIBER LASER RAMAN SENSOR

FOR CRYOGENIC APPLICATION

By

Appolinaire Tifang Luanje

Approved:

Jagdish P. Singh Adjunct Professor of Physics and Research Professor in Institute For Clean Energy Technology (Director of Thesis)	David L. Monts Professor of Physics and Graduate Coordinator of the Department of Physics and Astronomy (Committee Member)
Chuji Wang Assistant Professor of Physics (Committee Member)	Gary L. Myers Interim Dean of the College of Arts & Sciences

Name: Appolinaire Tifang Luanje

Date of Degree: May 3, 2008

Institution: Mississippi State University

Major Field: Physics

Major Professor: Dr. Jagdish P. Singh

Title of Study: INTEGRATED OPTICAL FIBER LASER RAMAN SENSOR FOR CRYOGENIC APPLICATION

Pages in Study: 35

Candidate for Degree of Master of Science

An integrated fiber optical Raman sensor was designed for real-time, non – intrusive detection of liquid and gaseous mixtures at high pressure and high flow rates. The integrated sensor employs a high-power solid-state pumped Nd:YAG frequency doubled (532nm) laser (3W), a modified In Photonics Raman probe which has built-in Raman signal filter optics, and two high-resolution spectrometers and photomultiplier tubes (PMT) with selected bandpass filters to collect both N_2 and O_2 Raman signals. The detection unit was also integrated with Lab View software interfaced PMT modules for fast data acquisition.

DEDICATION

I will also like to dedicate this research to my family, who offered me unconditional love and support throughout the course of this thesis.

ACKNOWLEDGEMENTS

I will also like to express my gratitude to my supervisor, Dr. Jagdish P. Singh, whose expertise, understanding, and patience, added considerably to my graduate experience. I appreciate his vast knowledge and skill in many areas. I would like to thank the other members of my committee: Dr. David L. Monts and Dr. Chuji Wang for the assistance they provided at all levels of research and class work.

I am indebted to Mrs. Fang-Yu Yueh for providing me direction and assistance during the research work. I am thankful to Dr. Rajamohan R. Kalluru for fruitful discussions and guidance. A special thanks to Mr. Vidhu S. Tiwari and Mr. Tracy S. Miller for being supportive and constantly encouraging me to realize my research goals. I am also thankful to Mr. Amitava Moitra and other colleagues for being helpful on various occasions. Thanks also goes out to all faculty and staff of the Department of Physics and Astronomy and all personnel in the Institute for Clean Energy Technology.

In conclusion, I recognize that this research would not have been possible without the financial assistance of NASA/SSC STTR.

TABLE OF CONTENTS

	Page
DEDICATION	ii
ACKNOWLEDGEMENTS	iii
LIST OF FIGURES	v
CHAPTER	
I. INTRODUCTION	1
1.1 Application of Optical Fiber	2
1.2 Aims and Objectives	3
II. SPECTROSCOPY	6
2.1 Definition of Spectroscopy	6
2.2 Raman Spectroscopy	6
2.3 Principles of Raman Spectroscopy	8
2.4 How Does Raman Spectroscopy Work	9
2.5 Other Forms of Raman Spectroscopy	10
III. EXPERIMENTAL SETUP AND DETAIL	11
IV. RESULTS AND DISCUSSION	24
V. CONCLUSIONS	32
REFERENCES	33

LIST OF FIGURES

FIGURE		Page
1.1	Schematic of liquid oxygen LOX feed line tank	4
2.1	Vibrational mode of diatomic molecules	7
2.2	Schematic illustration of classical and quantum mechanical explanation of scattering	9
3.1	Melles Griot Nd: YAG laser	12
3.2	High-resolution Ocean Optics QE65000 scientific-grade spectrometer	13
3.3	Schematic of the experimental setup using gaseous mixtures	14
3.4	Schematic of the experimental setup using liquid mixtures	15
3.5	Photomultiplier tube (Hamamatsu Model R955)	16
3.6	Photomultiplier tube (Hamamatsu Model H6776-20)	16
3.7	Photomultiplier tube (Hamamatsu Model R928)	17
3.8	Raman signal splitter into three detection units	18
3.9	Raman signal splitter into two detection units	18
3.10	Schematic of the experimental setup using liquid and gaseous samples	19
3.11	In-Photonics Raman probe (RPB532)	20
3.12	Schematic of the focusing and filtering optics within the Raman probe	20
3.13	Schematic of the integrated Raman sensor system	21
3.14	Photograph of the complete integrated Raman sensor system	22

3.15 Sensor system top level components 23

3.16 Sensor system bottom level components 23

3.17 The Raman sensor system with two probes and two laptops..... 23

4.1 Raman spectrum of gaseous nitrogen (400psi) & oxygen (300psi) mixture 25

4.2 Raman spectrum of 100gm liquid oxygen and 150gm of liquid nitrogen 26

4.3 PMT response to liquid nitrogen to different concentration ratios of liquid nitrogen and liquid oxygen mixture..... 28

4.4 Peak intensity ratio of LN2/LO2 against the weight ratio of LN2/LO2 using QE65000 spectrometer detection system 29

4.5 Voltage signal of N_2 and O_2 and their ratios 30

4.6 PMT voltage ratio of LN_2/LO2 vs. LN_2/LO2 concentration ratios 31

CHAPTER I

INTRODUCTION

The light guiding principles behind optical fibers was first demonstrated by Daniel Colladon and Jaques Babinet in the 1840s, with the Irish inventor offering public displays using water fountains ten years later. In 1952 physicist Narinder Singh Kapany conducted experiments that led to the invention of optical fibers.[1] An optical fiber is a cylindrical dielectric waveguide that transmits light along its axis, through the process of total internal reflection. An optical fiber consists of a core surrounded by a cladding layer. In order to confine to the optical signal inside the core, the refractive index of the core must be greater than of the cladding. Optical fibers are used in imaging optics whereby a coherent bundle of fibers is used, sometimes along with lenses for an image device called endoscope, which is used to view objects through a small hole. An optical fiber doped with certain rare earth elements, such as erbium can be used as a gain medium of a laser or optical amplifier. An optical fiber could also be used to supply low-level power (around one watt) to electronics situated in harsh electrical environment. Examples of these are electronics in high-powered antenna elements and measuring devices used in high voltage transmission.

1.1 Applications of Optical Fibers

Optical fibers can be used as a medium for telecommunication and networking because it is flexible and can be bundled as a cable. Since light propagates through optical fibers with little attenuation, optical fiber are especially advantageous for long-distance communications.[2] Additionally light signals propagating in the fiber can be modulated at rates as high as 40Gb/s and each fiber is capable of carrying many independent channels, each at different wavelengths of light. Since optical fibers are non-electrical, fiber cables can be used in environments where explosive fumes are present without danger of explosion. They are also immune to electrical interference; this prevents cross-talk between signal in different cables and pickup of environmental noise. Although fibers can be made out of transparent plastic, glass, or a combination of the two, the fibers used in long-distance telecommunication are always glass because of the low optical attenuation.[3]

Fiber optics also have application in medicine; the initial effort in fiber optics was concerned with the fabrication of aligned flexible fiber bundles for endoscopic visualization of the internal portions of the human body. As a result of the advancements of optical fiber technology, flexible fiberscopes have been applied not only to gastroscopy, but also to other areas of endoscopy, such as rectoscopy, laparoscopy, cystoscopy, etc. The application of lasers in the field of retinal coagulation [4-5] has pointed to the possibility of combining fiber optics and lasers for the remote coagulation of tissues.[6]

The area of fiber optical technology is receiving much attention in the military; it is being used for data transmission in aircraft. A point-to-point fiber optics link carries information between computers, sensors, and systems on board aircraft. This system is very attractive because it is small, light weight, free from electromagnetic interactions, and also free from impedance-matching problems. This area of optical technology is receiving a lot of attention from industries as well and from the military point of view this technology can offer unique solutions to critical problems.[7]

Optical fibers can also be used as sensors to measure strain, pressure, temperature, humidity, vibration, cracks, etc. Optical sensors have certain advantages over electrical sensors due to their smaller size and also due to the fact that no electrical power is needed at remote locations. Hydrophones for seismic or SONAR applications uses optical fibers; this sensor systems is used by oil industries as well as countries navies. The German company Sennheiser, developed a microphone that works with a laser and optical fibers.[3] Optical fiber sensors for temperature and pressure measurement have been developed for downhole measurements in oil wells. Fiber optical sensors have been developed to measure temperature and strain simultaneously with very high accuracy.[8] This is a particularly useful way to acquire information from complex structures.

1.2 Aims and Objectives

Our goal is to design an integrated online real-time fiber optical sensor which will be capable of monitoring and measuring the concentration ratios of cryogenic liquid oxygen (LOX) during rocket engine testing. A flow of pressurized liquid nitrogen

maintains the tank pressure and also forces liquid oxygen from the tank to the test engine. Figure 1.1 below shows the schematics of LOX feed line and LOX tank. Liquid nitrogen boils at −195.79° C (-320.42° F), and oxygen at −182.96° C (-297.33° F).

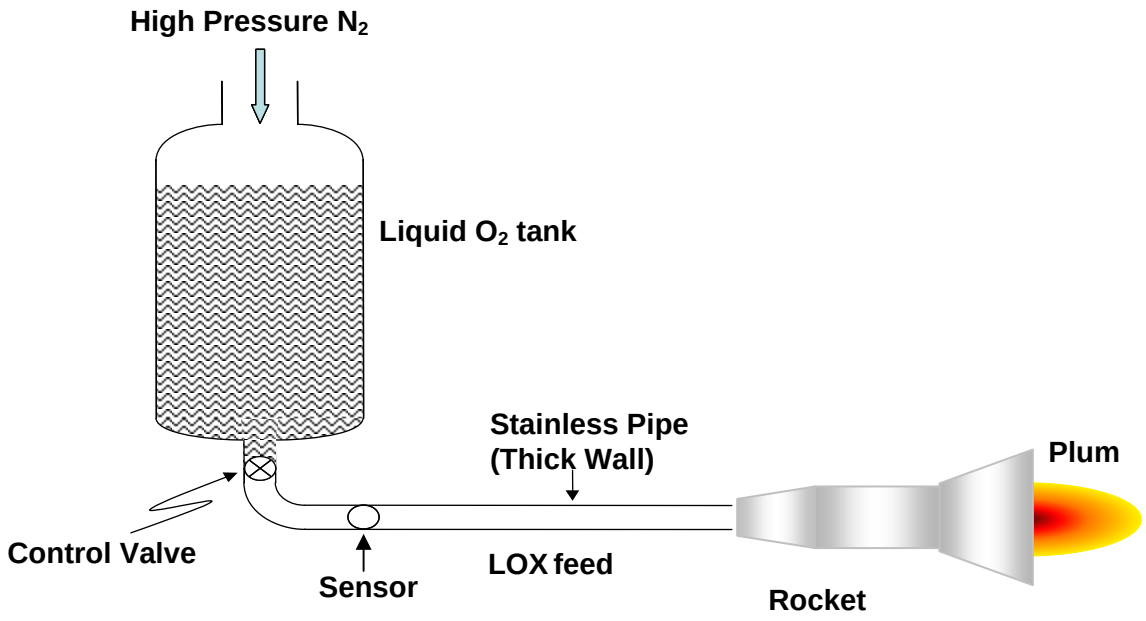

Figure 1.1: Schematic of liquid oxygen LOX feed line tank. [25]

Liquid nitrogen LN_2 mixes with liquid oxygen LOX and as the test runs to an end there will be some nitrogen contamination in the liquid oxygen supplied to the engine. Monitoring the concentration ratio of LN_2/LOX becomes quite important. The typical run time of an engine test is 10-30 seconds. The time response of the sensor should be 10-1000 milliseconds depending on the specific engine test. The fast time response of the

sensor will be used to design a control to shut down the test as soon as the impurity of liquid nitrogen exceeds a certain threshold level.

This sensor uses the principle of Raman spectroscopy. Spontaneous Raman spectroscopy (SRS) has been known for several years as a very simple analytic method for identification of solids, liquids, and gaseous molecules by the laser light scattered by these molecules.[9-18] With the use of photomultiplier tube (PMT) as a detector, our integrated system is capable of producing of producing milliseconds response time of the sample under investigation. Since our integrated system is relatively simple, non-intrusive, very sensitive, and easily portable it is very suitable for field application.

The Raman sensor consist of four major components namely the excitation source, the sample illumination and light collection optics, wavelength selectors, and the detectors. Each component for the sensor was selected and the various optical components were aligned. The components in the integrated sensor were tested individually in order to verify the functionality of each part. Samples of gaseous and liquid mixtures were prepared with various concentration ratios. With the spectrometer detector, we were capable of obtaining Raman spectra of liquids at varying concentrations under the same experimental conditions. The spectrometer as a detector provides a wide-band Raman spectrum with a response time of seconds/sub-seconds for the sample under investigation. Since the sensor system has to record fast data acquisition in the range of milliseconds, PMT was chosen for detection. Finally the spectral data are processed using a computer.

CHAPTER II

SPECTROSCOPY

2.1 Definition of Spectroscopy

Spectroscopy has been used to determine the molecular composition of a wide range of complex samples, including liquids, solids, and gases. It is basically the interaction of light with matter. The measurement of this interaction is known as spectrometry and the instrument used in performing such measurement is known as spectrometer or spectrograph. There are several types of spectroscopy techniques namely; Raman, laser induced breakdown, fluorescence, luminescence, near infrared (NIR), microwave, X-ray, gamma ray, infrared, ultraviolet, absorption, reflection, and transmission spectroscopy. Raman spectroscopy is used in this work. The details of Raman spectroscopy are given below.

2.2 Raman Spectroscopy

It is an analytic technique based on the detection of scattered light and is used for a variety of applications involving solids, liquids and gases. Raman spectroscopy probes the vibration modes of materials, much like infrared (IR) spectroscopy. Figure 2.1 below shows the vibrational mode of diatomic molecules. However, whereas IR bands arise from a change in the dipole moment, Raman bands arise from a change in the polarization of the molecule. In many cases, such as N_2, O_2, and H_2, transitions that are

allowed in Raman spectroscopy are forbidden in IR, so these techniques are often complementary. If a molecule has a center of symmetry, then no modes of vibration can be both infrared and Raman active.

The basis of this technique is monitoring scattered light from an irradiated sample. A small portion of the scattered light exhibits a slight shift in wavelength due to molecular vibrations of the sample. Using this wavelength shift, the sample could be analyzed. This spectroscopic technique has been used for many years to investigate various molecules, including biological molecules, In recent years, it has been used mostly in diagnostics[20-22] and most of the diagnostic applications are still in their early stages of development.[19]

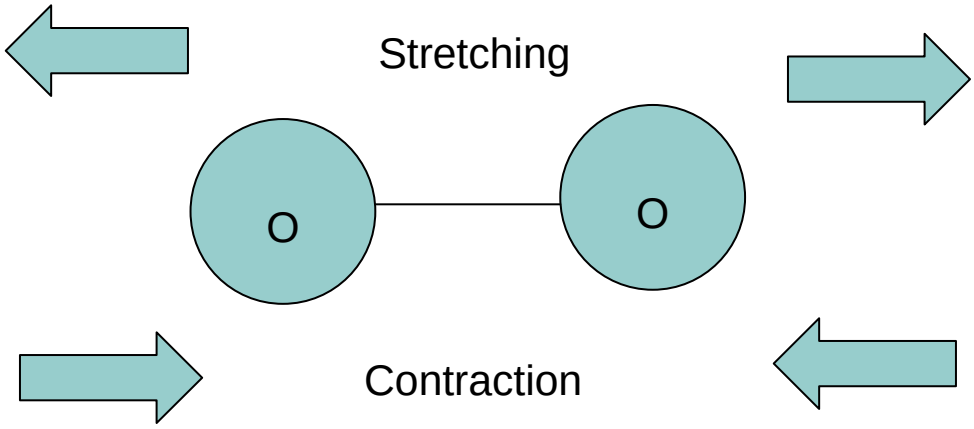

Figure 2.1: Vibrational mode of diatomic molecules.

2.3 Principles of Raman Spectroscopy

Raman spectroscopy is based on the Raman effect, which results from the exchange of energy between incident photons and scattering molecules. When the energy of the incident photon remains unchanged after collision with a molecule, the scattered photon has the same frequency as the incident photon. This is known elastic or Raleigh scattering. When the scattered photon has more (or less) energy than the incident photon, it is known as inelastic or Raman scattering, as shown in Figure 2.1. Quantum mechanically, Raman spectroscopy is a result of an energy transition of the scattering molecule to a virtual excited state and its return to a higher (or lower) vibrational state with the emission of an altered incident photon. The scattered photon can have more (or less) energy than the incident photon since energy can be transferred either from the photon to the molecules of from the molecule to the photon. Raman Stokes scattering is observed when the scattered photon has less energy than the incident photon: Raman anti-Stokes scattering is when the scattered photon has more energy than the incident photon. A Raman spectrum is a plot of scattered intensity as a function of the frequency shift. The frequency shift represents the characteristics of the molecule which collided with the photon, the resulting spectrum is characterized by a series of Raman bands which correspond to the vibrational modes of the molecule.[19] Since Raman signals are usually very weak, powerful lights sources and sensitive detectors are required.

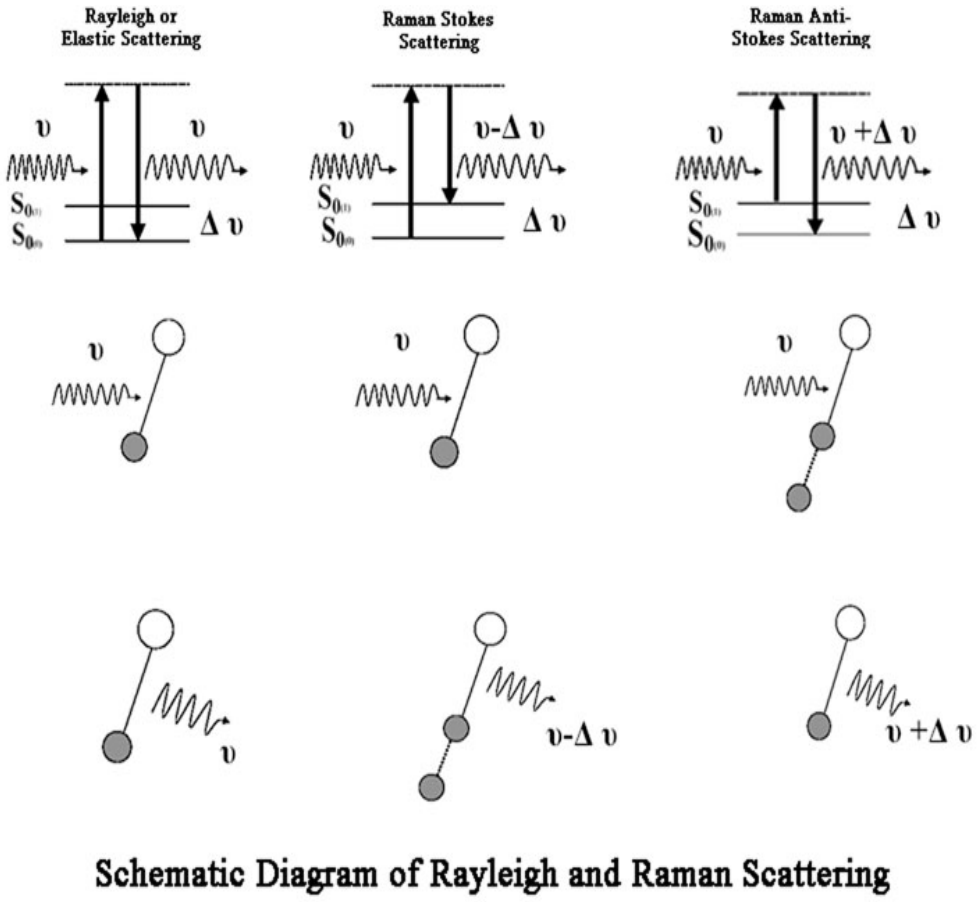

Figure 2.2: Schematic illustration of classical and quantum mechanical Explanation of scattering [19]

2.4 How Does Raman Spectroscopy Work

The basic components for Raman spectroscopy include a light source (laser), collection optics to gather the Raman-scattered light, and a detection system. For biomedical applications, it is usually recommended to work with laser light in the near-infrared to minimize problems with tissue fluorescence and tissue damage. Raman spectroscopy can be described as shining light onto a sample and investigating the

interaction between this light and the chemical bonds in the sample. This interaction is what is known as the Raman effect.

2.5 Other Forms of Raman Spectroscopy

There are many other forms of Raman spectroscopy.[22] Some of these different techniques are a being carried out by research groups around the world. Some of these forms of Raman spectroscopy are:

(1) Surface Enhance Raman Spectroscopy (SERS)

(2) Laser Raman Scattering (LRS)

(3) Raman Optical Activities (ROA)

(4) Time-resolved Raman scattering

(5) Coherent Anti-Stokes Raman Scattering (CARS)

CHAPTER III

EXPERIMENTAL SETUP AND DETAILS

This research effort builds on previous work carried out by Tiwari *et al*.[28], where a low-resolution spectrometer and an inexpensive laser diode were used to develop a prototype sensor for monitoring the concentration of LN_2 and LOX in a cryogenic mixture.

The Raman sensor was set up using a frequency-doubled 532-nm continuous wavelength (CW) multimode neodymium: yttrium aluminum garnet (Nd: YAG) laser (Melles Griot GHS 309) as the excitation light source. The maximum output power was 3W. The laser could be operated at different power in the range of 0.01-3W. The laser line width was approximately 0.18nm and beam diameter approximately 0.24mm. Figure 3.1 below shows the Melles Griot laser.

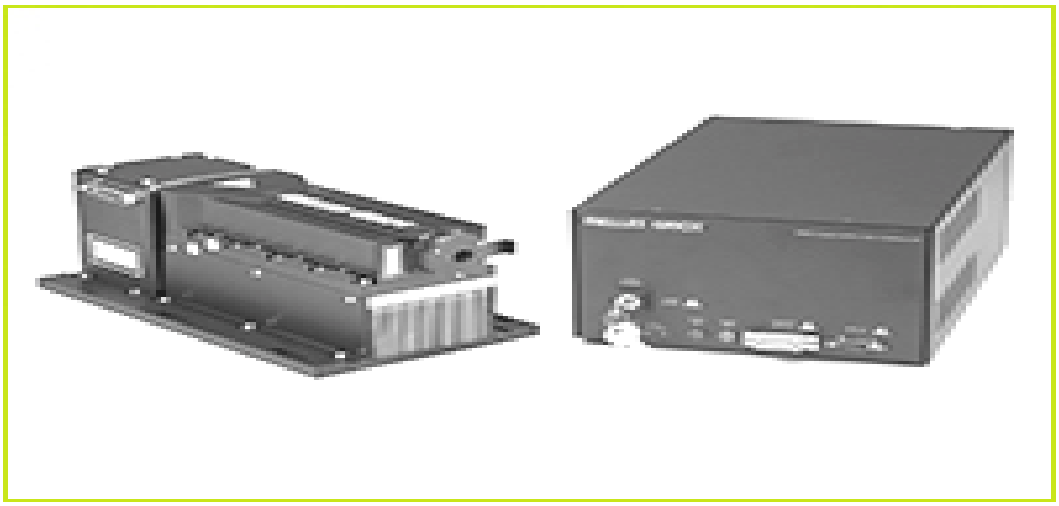

Figure 3.1 Melles Griot Nd: YAG laser.[24]

A convex lens of focal length 2cm was used to focus the laser light onto the tip of In Photonics Raman probes (RPB532). . Sensor configurations were employed with two modified In Photonics fiber optics state-of-art miniaturized Raman probe (RPB532) which consists of just two parallel optical fibers. One fiber (105-μm core diameter) was used for guiding the launched light to the sample. The other fiber (200-μm core diameter) collected the emitted Raman signal. The In-Photonic probe had a built-in optics to attenuate the scattered laser light (Raleigh scattering) and also to filter the Raman signal fed into the detection unit. An Ocean Optics QE65000 scientific –grade spectrometer with combination of detector, optical bench, and electronics served as the detection unit for monitoring the Raman signal of liquid nitrogen and oxygen mixtures. This system was chosen because of its low light detection capability. The spectrometer has a grating of 1200 1/mm which covers 540-710nm wavelength region. With this QE65000 spectrometer, up to 90% quantum efficiency can be achieved with a high signal-to-noise

ratio and rapid signal processing speed.[23] A photograph of a QE65000 spectrometer is shown in Figure 3.2.

Figure 3.2: High-resolution Ocean Optics QE65000 scientific-grade spectrometer.[23]

The spectrometer has a 1024-element charge coupled device (CCD) attached to the exit of the spectrograph, and was interfaced to a personal computer (PC) via a USB port. Experimental setups for these measurements are shown in Figures 3.3 and 3.4. The spectrometer was used as a detection unit to identify the Raman wavelength of N_2 and O_2 in order to compare their relative signal strengths.

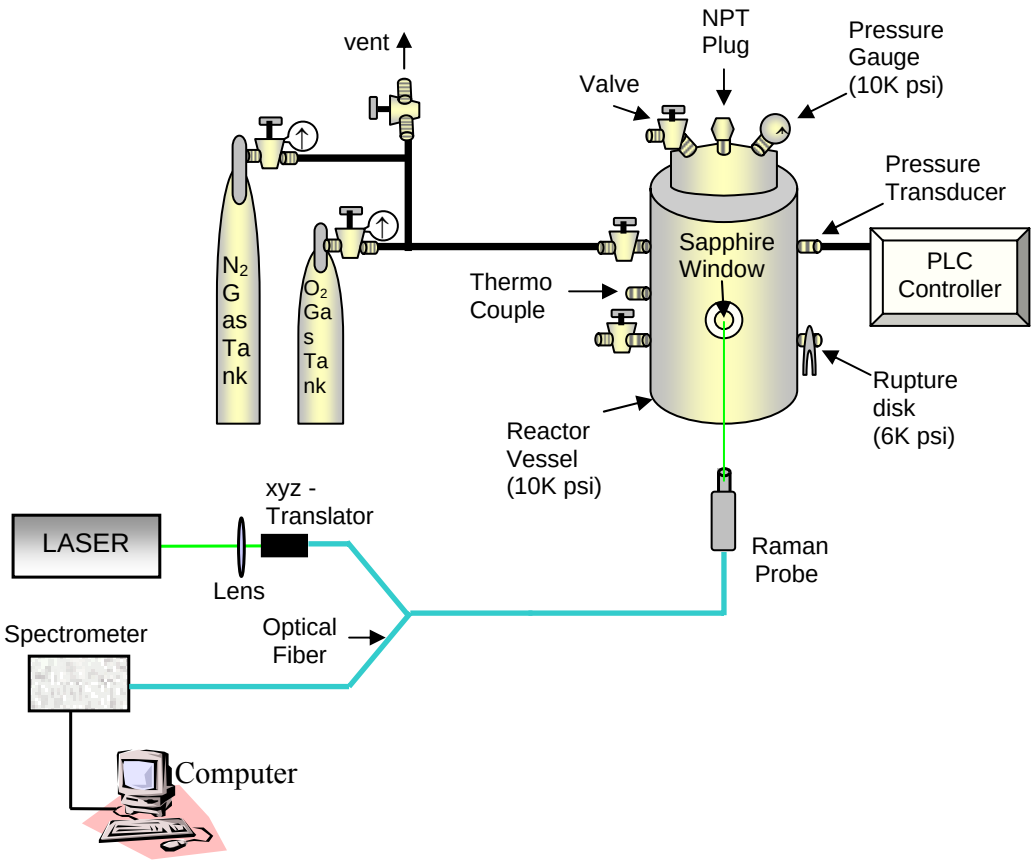

Figure 3.3: Schematic of the experimental set up using gaseous mixture.[25]

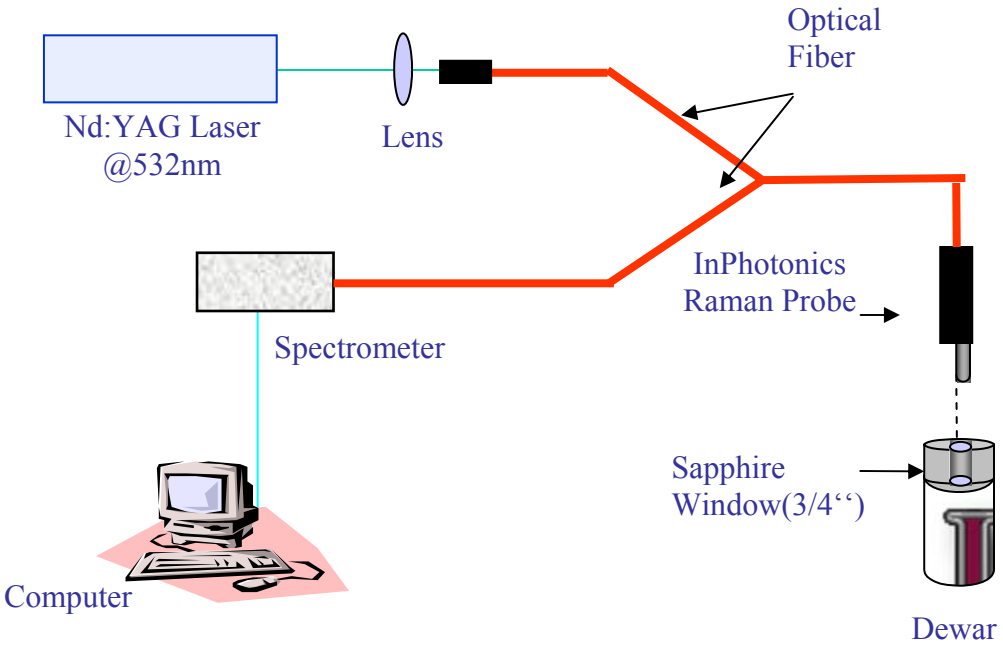

Figure 3.4: Schematic of the experimental set up using a liquid mixture.[28]

To improve the response time of the sensor and for real-time monitoring of our sample under investigation, a photomultiplier tube (PMT) based detection system is also integrated into the sensor configuration. At the initial stage, we used the photomultiplier tube (Hamamatsu model R955) shown is Figure 3.5 below. Because of the external high power voltage supply, the PMT was very bulky for use in the integrated sensor system

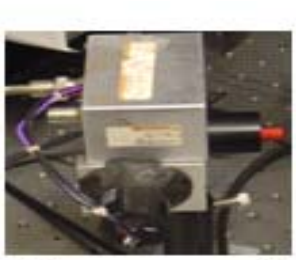

PMT (Hamamatsu # R955) in an shielded enclosure

High Power Voltage Supply (HPVS)

Figure 3.5 Photomultiplier tube (Hamamatsu Model R955)[24].

. The next stage was getting a more compact, integrated PMT/HVPS and a wider spectral range (300nm-900nm) as shown is Figure 3.6 below. This PMT contains a signal amplifier with low-pass noise filter and a 10-kΩ potentiometer which adjusts the PMT sensitivity.

Figure 3.6 Photomultiplier tube (Hamamatsu Model H6776-20). [24]

Several experiments were conducted in the laboratory with this PMT (Model H6776-20), but the Raman signal was very weak. The weak Raman signal was due to the small diameter (8mm) side-on PMT window and also the fact that this PMT is not as sensitive to the Raman signal as the previous PMT (R955).

Finally, another compact PMT (model R928) with a much larger side-on window (24mm diameter) was purchased from Hamamatsu. This PMT (model R928) was very sensitive in the spectral region between 185nm and 900nm and also had an integrated power supply.[24] Figure 3.7 below shows this PMT (model R928).

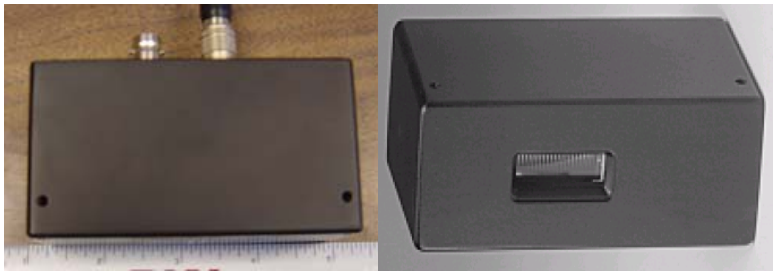

Figure 3.7: Photomultiplier tube (Hamamatsu Model R928).[24]

The emitted Raman signal is coupled into the PMT using suitable bandpass filters to only detect N_2 or O_2 Raman signals. The PMT converts the light signal into a current, which is then converted to voltage by a built-in current-to-voltage converter.

I attempted on to separate the Raman signal into three detection units, but the split Raman signals were very weak and could not be detected. The next step was to seperate

the signal into two detection units. The diagram of the Raman signal splitter is shown in Figures 3.8 and 3.9 below.

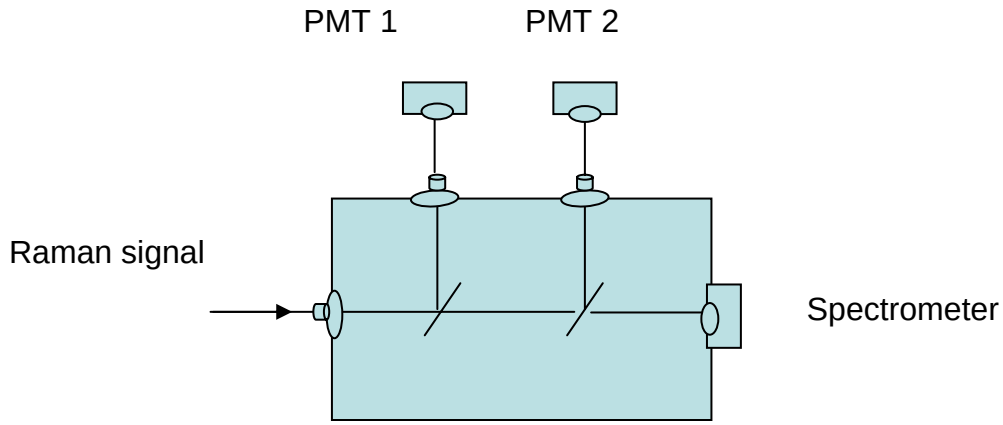

Figure 3.8: Raman signal splitter into three detection units.

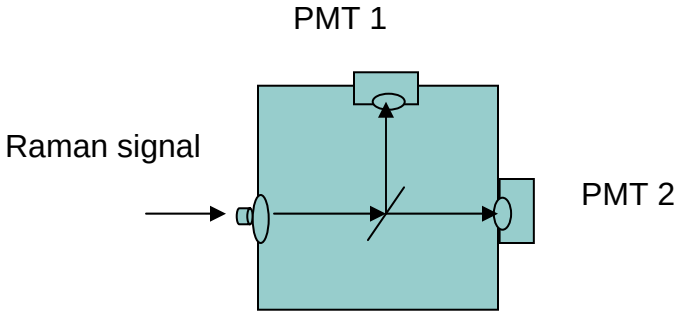

Figure 3.9: Raman signal splitter into two detection units.

The voltage output signal of each PMT was separately fed to the computer via a data acquisition board (DAQ board SCB-68). For data storage and data analysis purposes, the Lab View 7.1 software (from National Instruments) was used. A PMT-

based detector has proven to be more suitable for estimating the Raman signal of N_2 and O_2 and provides a fast response time. The experimental setup is shown is Figure 3.10.

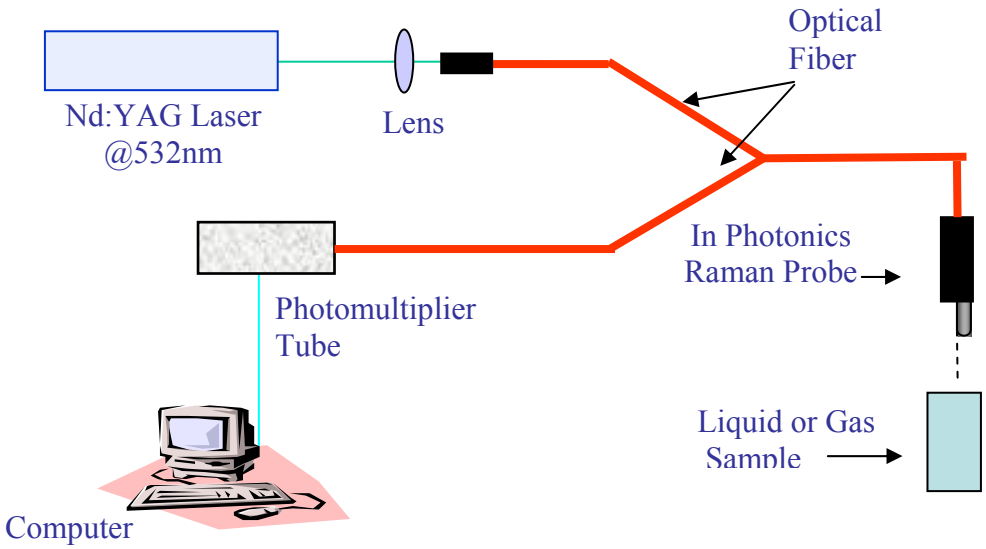

Figure 3.10: Schematic of the experimental set up using liquid and gaseous samples.

The In Photonics Raman probe (RPB532) is lightweight and compact and has a very flexible probe-head. It is equipped with filters that reduce the backscattered laser signal below the intensity of the Raman signal. As a result of this filtering, the detector is free from saturation of unwanted laser light. A photograph of the InPhotonic probe is shown in Figure 3.11. A schematic of the optics aligned in the probe is shown in Figure 3.12.

Figure 3.11: In-Photonics Raman probe (RPB532).[25]

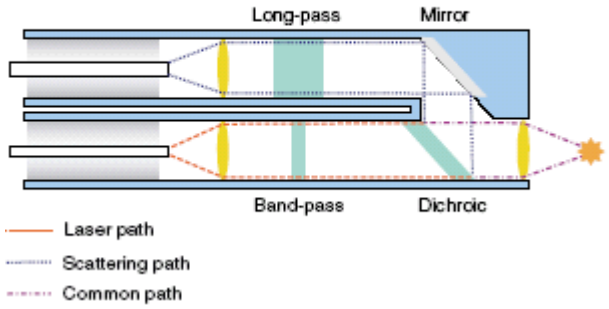

Figure 3.12: Schematic of the focusing and filtering optics within the Raman probe.[25]

After the initial testing of the above individual sensor component, a complete integrated Raman system was designed for real time field application and the setup is shown in Figure 3.13. In this system, the laser light was separated into two beams using a 50/50 beamsplitter. The laser light was then coupled into the In-Photonics probe through collimating lenses. The integrated Raman sensor system is capable of analyzing liquid and gaseous samples simultaneously with the two fiber optical Raman probes in place. Two computers are employed with the integrated Raman system, one is used for the laser

operation and data collection from the PMT and the other is used to collect data from the Ocean Optics spectrometer.[25]

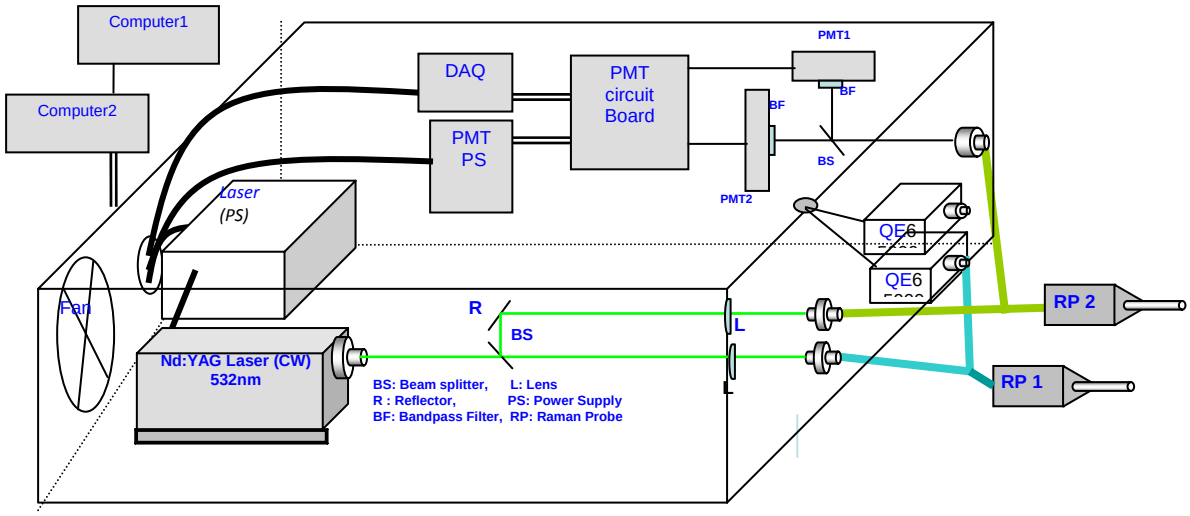

Figure 3.13: Schematic of the integrated Raman sensor system.[29]

The uniqueness of the sensor lies in its compact design configuration, which includes filter holders, PMT, DAQ board with electronic circuit boards, spectrometers, carefully aligned optical components, and high-power laser. A fan which is built-in to the laser power supply is assembled to facilitate air circulation inside the prototype box. The air circulation helps to maintain an optimum temperature within the prototype box. Figure 3.14 is a photograph of the integrated Raman system box.

Fig. 3.14: Photograph of the complete integrated Raman sensor system.

The sensor box is consists of two levels. The top level contains the laser system and the carefully aligned optically components. The arrangement of the components of the top level is shown in Figure 3.15. The bottom level consists of the power supplies that are required to operate the different components. The arrangement of the components on the bottom level is shown in Figure 3.16. Figure 3.17 shows the two Raman probes, the sensor box, and two laptop computers for data analysis.

Figure 3.15: Sensor system top level components.

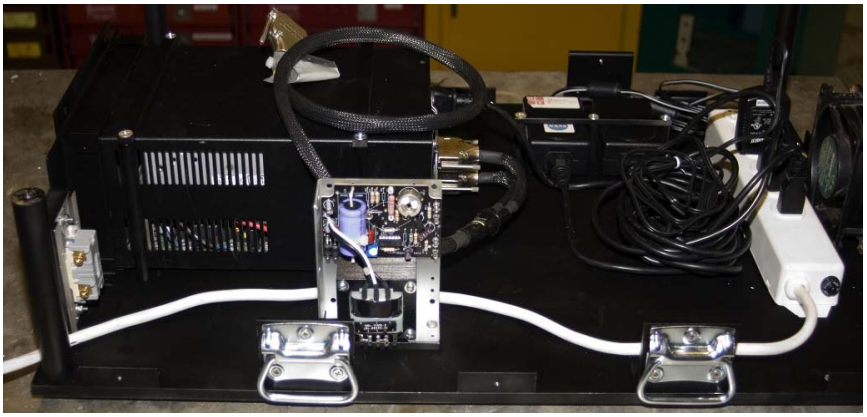

Figure 3.16: Sensor system bottom level components.

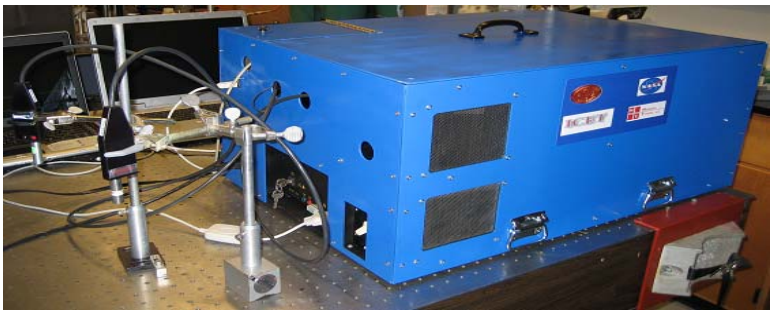

Figure 3.17: The Raman sensor system with two probes and two laptops.

CHAPTER IV

RESULTS AND DISCUSSION

The aim of work is to monitor the concentration of liquid nitrogen in liquid oxygen without disturbing the flow rate of liquid oxygen. As a result of this, a non-intrusive, highly sensitive, online monitoring, and rapid collection time frame fiber optical Raman sensor has been developed. We used gaseous mixtures in the initial detection phase because these mixtures are more stable and can be used for sensor calibration. In the past, Raman spectra of gaseous mixtures of nitrogen and oxygen have been studied with a low resolution spectrometer in our lab.[30] Based on the previous work, Raman spectra of gaseous mixtures of nitrogen and oxygen were recorded, but this time with a high-resolution Ocean Optics Inc (OOI) spectrometer (QE65000). Figure 4.1 shows a Raman spectrum of gaseous mixture of nitrogen (400psi) and oxygen (300psi). The Raman spectra were recorded with an integration time of 300ms and average of 10 spectra, resulting in a 3-sec data acquisition recording time.

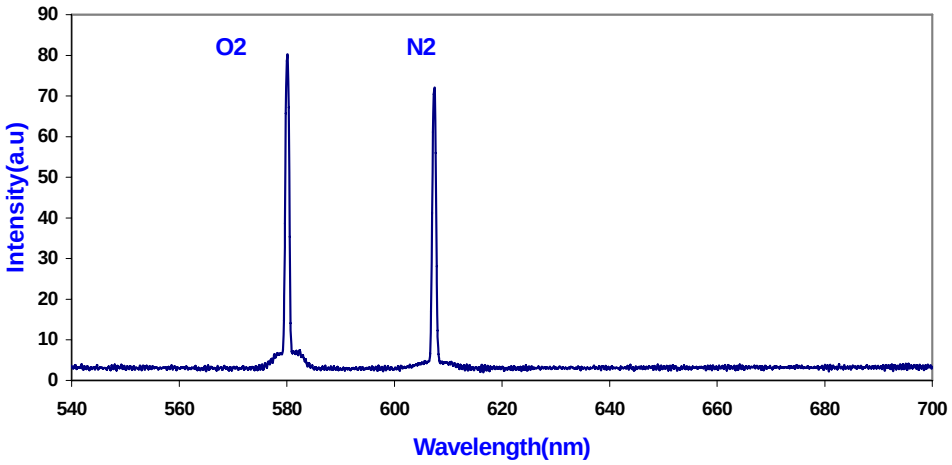

Figure 4.1: Raman spectrum of gaseous nitrogen (400psi) & oxygen (300psi) mixture.

Experiments were carried out using different concentration ratios of liquid nitrogen and liquid oxygen. The Raman spectra for these mixtures were recorded with an integration time of 300ms and then ten spectra were averaged, resulting in a 3-sec data acquisition time. Owing to the fact that we were working with cryogenic liquid with a very high vaporization rate, we tried to minimize the vapor loss by mounting a cap with a hole on the top of the Dewar in order to maintain the nitrogen-to-oxygen ratio in the mixtures.

Though the hole allowed clear passage for laser light, it could not prevent the condensed liquid from escaping and condensing on the tip of the Raman probe. In order

to be more accurate with our results, we had to determine the rate of evaporation of the cryogenic liquid mixture, which was found to be approximately 1.4 g/min. A quartz window was introduced inside the cap hole to provide optical access for the laser beam to interact with the cryogenic mixtures. As a result of this, there was approximately 5% reduction in the evaporation rate of the cryogenic liquid mixture. With all these conditions in place, the sample mixture was prepared by adding liquid oxygen to liquid nitrogen. Due to the fact that the molecular weight of oxygen is more than that of nitrogen, the evaporation rate of liquid nitrogen was highly suppressed.[13] The Raman spectrum for a 40% liquid oxygen and 60% liquid nitrogen mixture is shown in Figure 4.2. Raman bands of oxygen (580nm) and nitrogen (607nm) with corresponding Raman shifts for oxygen (1556.4cm^{-1}) and nitrogen (2330.7cm^{-1}) is represented in the spectrum.

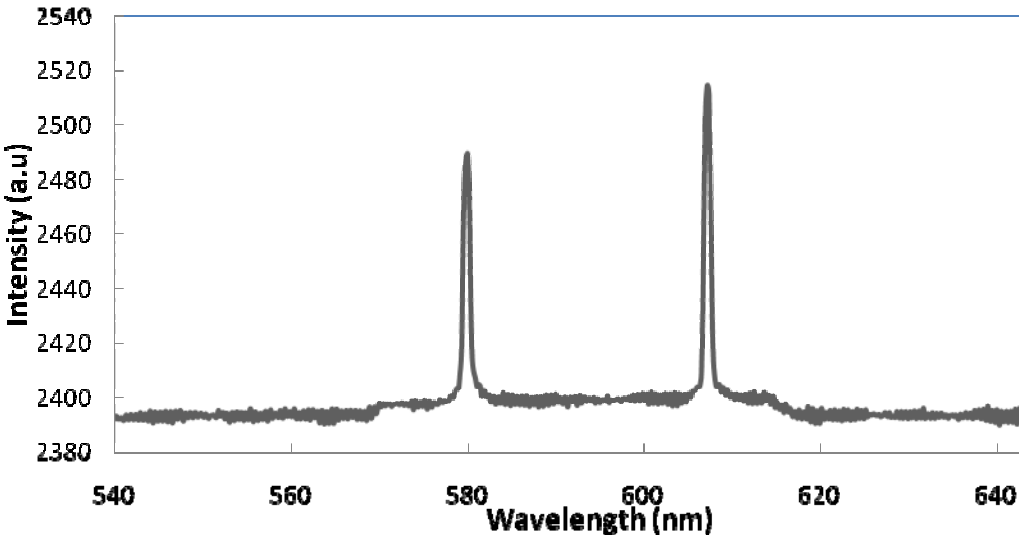

Figure 4.2: Raman spectrum of 100gm liquid oxygen and 150gm of liquid nitrogen.

For fast data acquisition, we employed a PMT-based detection system. The Raman signal was converted into an electrical signal with the aid of the PMT which is sensitive to light in the ultraviolet, visible and near infrared regions. The main idea of using PMT was to amplifier the weak Raman signal and also to improve the sensor response time for fast data acquisition. A 610-nm (±10 nm) bandpass filter was employed to transmit only the nitrogen signal and a 580-nm (±10 nm) bandpass filter for oxygen signal. The concentration ratio of liquid nitrogen in liquid oxygen mixture was also monitored. The data acquisition time was 10ms, which is much shorter than that of the spectrometer. From Figure 4.3, it can be seen that the concentration ratio of liquid nitrogen with respect to liquid oxygen increased by a factor of ~2 in the liquid mixture. The signal was very unstable because of the rapid phase transforming nature of cryogenic liquid mixtures.

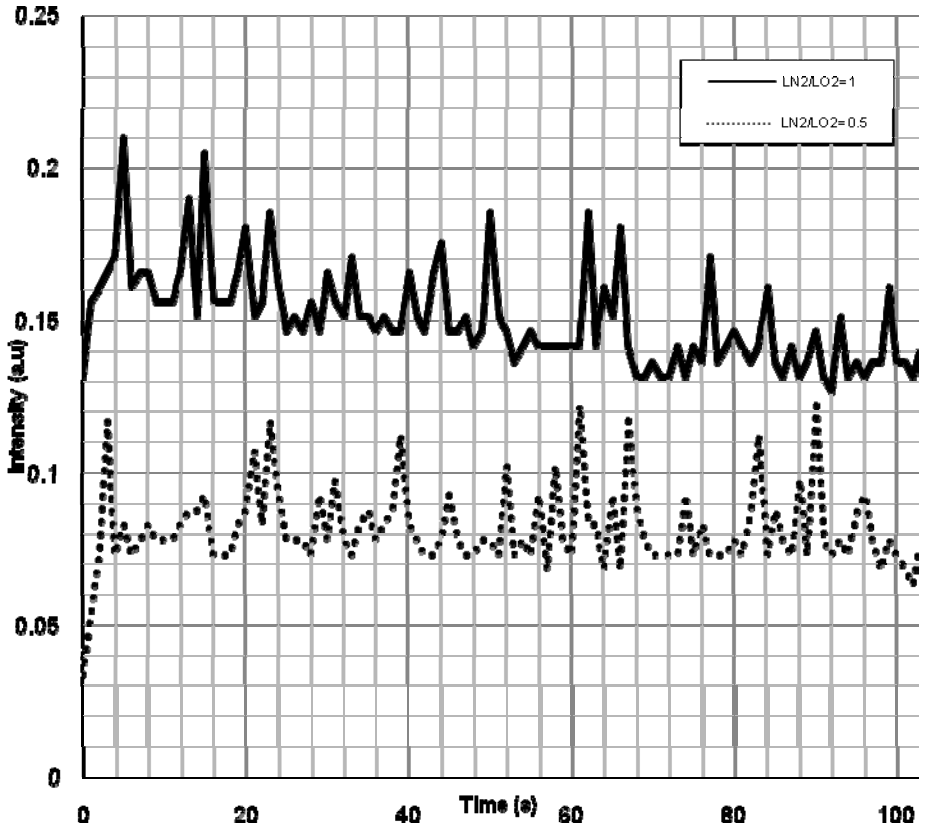

Figure 4.3: PMT response to liquid nitrogen to different concentration ratios of Liquid nitrogen and liquid oxygen mixture

After the initial testing of the individual components of the sensor box, we had to assembly an integrated fiber optical sensor which has the capability of multiphase (liquid and gaseous phases) and ultra-fast detection of samples under investigation. Tests with cryogenic mixtures of liquid nitrogen and liquid oxygen were carried out. With the spectrometer detection unit, Raman signals of liquid nitrogen and liquid oxygen were analyzed in terms of their signal-to-noise ratio, peak intensity, etc. The Raman peak intensity ratios of liquid nitrogen and liquid oxygen at various weight ratios were calculated and a calibration curve was obtained as shown in Figure 4.4.

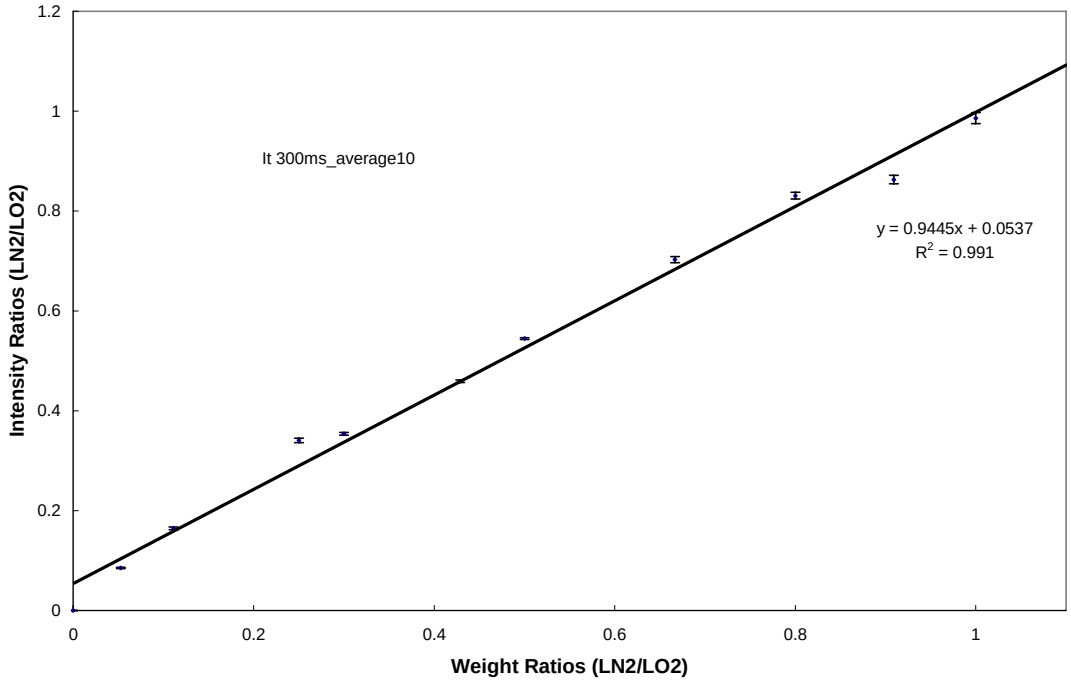

Figure 4.4: Peak intensity ratio of LN2/LO2 against the weight ratio of LN2/LO2 Using QE65000 spectrometer detection system

From Figure 4.4 above, we can see a linear trend in liquid nitrogen and liquid oxygen concentration ratio between 0.1 and 0.9. There is saturation above this range due to rapid phase change occurring in these cryogenic liquids.

For fast data acquisition, a PMT detection system was used. The voltage from two the PMTs and their corresponding liquid nitrogen-to-liquid oxygen ratio can be seen using Lab View software in the figure below.

Figure 4.5: Voltage signal of N_2 and O_2 and their ratios.

A calibration curve was obtained with the variation of liquid nitrogen to liquid oxygen concentration against the concentration weight ratio of liquid nitrogen and liquid oxygen mixture as shown in Figure 4.6.

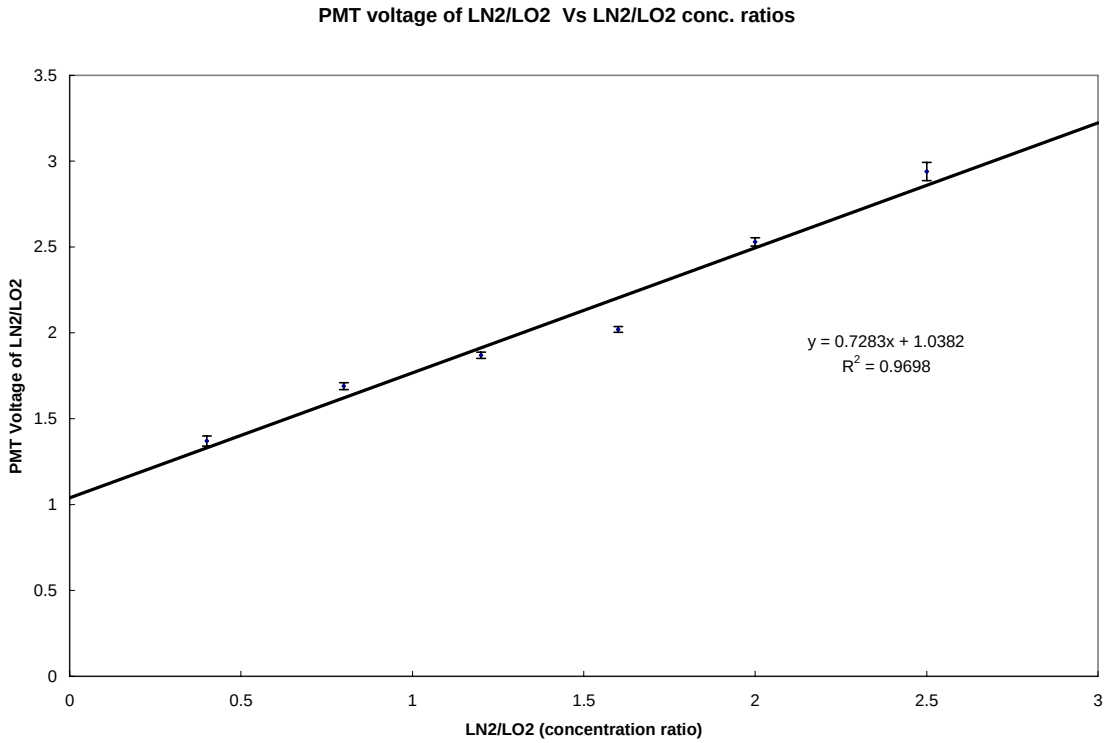

Figure 4.6: PMT voltage ratio of LN_2/LO2 vs. LN_2/LO2 concentration ratios.

CHAPTER V

CONCLUSIONS

This work presents a non-intrusive, highly sensitive, online, and real time, integrated fiber optical Raman sensor system for monitoring of cryogenic liquid and gaseous mixtures. Since Raman scattering is a very weak process, a high performance Raman optical sensor should have a good excitation source and a high-resolution and very sensitive detection system. With the availability of two Raman probes (In Photonic RPB-532), the integrated system can be used for dual detection, i.e., simultaneous monitoring of both the liquid and gas phases of samples under investigation. The two high-resolution spectrometers (QE65000) obtained from Ocean Optics, Inc could achieve up to 90% quantum efficiency with a high signal-to-noise ratio and could also enable low light-level detection with long integration time without any spectral saturation. We were capable of achieving an online, real time and rapid data acquisition integrated Raman sensor system with two highly sensitive, integrated PMTs (H6779) obtained from Hamamatsu. Raman spectra of liquids and gaseous mixtures obtained using the integrated sensor system where compared and there was a good correlation between the two phases. This sensor can also be applied to potential industrial applications, especially in quality control, rapid sensor response time and sensitivity, etc.

REFERENCES

[1] W.A. Gambling, IEEE Journal of Selected Topics in Quantum Electronics, Vol. 6, No 6(2000), P. 1084.

[2] J.D. Montgomery, IEEE Transactions on Communications, Vol. 26, No. 7 (1978), P. 1099.

[3] J.Gowar, Optical Communication Systems, Second Edition. , Prentice-Hall, Hempstead UK (1993).

[4] N.S. Kapany, N. Silbertrust, and N.A. Pepper, Applied Optics, Vol. 4, No. 5 (1965), P. 517.

[5] H.C. Zweng, M. Flocks, N.S. Kapany, N. Silbertrust, and N.A. Peppers, American Journal of Ophthalmology, Vol. 58 (1964), P. 353.

[6] N. S. Kapany, Fiber Optics Principles and Applications, Academic Press, New York (1967).

[7] R.A. Andrews, A.F. Milton, and T. G. Giallorenzi, IEEE Transactions on Microwave Theory and Techniques, Vol. 21, No. 12(1973), P. 763.

[8] J. Hecht, City of Light: The Story of Fiber Optics, Oxford University Press, New York (1999).

[9] D. Lin-Vien, N.B. Colthup, W.G. Fateley, and J.G. Grasselli, The Handbook of Infrared and Raman Characteristics Frequency of Organic Molecules, Academic Press, Boston (1991).

[10] B. Schrader, Raman and Infrared Atlas of Organic Compounds, Second Edition, VCH Verlagsgesellschaft, Wienheim (1989).

[11] R.A. Nyquist , C.L. Putzig, M.A. Leugers, R.O. Kagel, C.L. Putzi, and M.A. Leugers (eds), The Handbook of Infrared and Raman Spectra of Inorganic Compounds and Organic Salts, Vol. 1-4, Academic Press, San Diego (1997).

[12] R.A. Dluhy, S.M. Stephens, S. Widayati, and A.D. Williams, Spectrochimica Acta A, Vol. 51 (1995) P. 1413.

[13] C. Eckbreth, Laser Diagnostics for Combustion Temperature and Species, Second Edition, Gordon and Breach Publishers, Amsterdam , Chap. 5 and references therein(1996).

[14] K. K. Kuo and T. P. Parr, Non-intrusive Combustion Diagnostics, Begell House, Inc., New York (1994).

[15] D.A. Long, Raman Spectroscopy, McGraw-Hill, Inc., New York (1977).

[16] N.M. Laurendeau, Progess in Energy and Combustion Science, Vol. 14 (1988) P. 147.

[17] G. Zikratov, F. Y. Yueh, J. P. Singh, O. P. Norton, R.A Kumar, and R. L Cook, Applied Optics, Vol. 38 (1999) P. 1467.

[18] K. Kamogawa and T. Kitagawa, Chemical Physics Letters, Vol. 179(1991) P. 271.

[19] T. Vo-Dinh, Biomedical Photonics Hand Book, CRC Press, Boca Raton (2003).

[20] I.R. Lewis, and H.G.M. Edwards, Handbook of Raman Spectroscopy, First Edition, CRC Press, New York (2001).

[22] M.J. Pelletier, Analytical Applications of Raman Spectroscopy, Blackwell Science, U.K.(1999).

[23] http://www.oceanoptics.com/Products/qe65000.asp

[24] http://www.hamamatsu.com/

[25] J.P. Singh and F.Y. Yueh, "Real Time, Non-Intrusive Detection of Liquid Nitrogen in Liquid Oxygen at High Pressure and High Flow," NASA/SSC/STTR-Final Report Phase 2, Contract no. NNSO4AA34C.

[26] J.P. Singh and F.Y. Yueh, "Real Time, Non-Intrusive Detection of Liquid Nitrogen in Liquid Oxygen at High Pressure and High Flow," NASA/SSC/STTR-Final Report Phase 1, Contract no. NNSO5AB02C.

[27] V.S. Tiwari, R.R. Kalluru, F.Y. Yueh, J.P. Singh, W. S. Cyr, and S.K. Khijwania, Applied Optics, Vol. 46, No.16(2007), P. 3345.

[28] A.T. Luanje, R.R. Kalluru, V.S. Tiwari, F.Y. Yueh, J.P. Singh, W.S. Cyr, 37th AIAA Fluid Dynamics Conference and Exhibit, Miami (2007).

[29] V.S. Tiwari, S.K. Khijwania, F.Y. Yueh, J. P. Singh, R.R. Kalluru,, Oral Presentation 2250-10, PITTCON ,Orlando (2005).